60W Auxiliary Power Supply Demonstration board

1. DEMONSTRATION BOARD SUMMARY

The CRD-060DD12P is a Cree demonstration board for a single-end Flyback converter design with a commercially available 1700V Silicon Carbide (SiC) MOSFET to replace conventional two-switch Flyback converter for high voltage input auxiliary power supply of three phase applications. The demonstration board is not designed to be a product and is to be only used as a tool to evaluate the performance Cree switching devices.

2. INTRODUCTION

Three-phase applications, such as motor drive, UPS and PV inverter, have a front end AC/DC or DC/DC converter to boost the DC link voltage up to 600Vdc to 800Vdc. Factoring in a design margin, the maximum DC link voltage is up to 1000V. To support such systems in practice, an auxiliary power supply is used to generate power for cooling fans, displays, control logic and system protection functions with the DC link voltage as its input. For such low power applications, Flyback topology is the most common type in the industry; however, the conventional single end Flyback topology has difficulty in meeting high input voltage. The first difficulty is caused by the high input voltage (1000Vdc); the single-end Flyback topology would require high blocking voltage switching devices. Currently, the Silicon MOSFET only has 1500V blocking voltage, which has low voltage stress design margin and thus affects the reliability of the power supply. The second challenge is that most of the 1500V Si MOSFETs have very large on-state resistance, and this will lead to higher losses, higher thermal and lower efficiency, especially when the whole three-phase system is operating at light output load and auxiliary power losses occupy most of total system losses. Lastly, to support a wide input voltage range, a pure resistance start up circuit is normally used. However, the start-up resistance will lead to losses at high input voltage. Larger start-up resistance will have less losses but lead to long start-up time at low input voltage.
In order to overcome these auxiliary power supply design challenges to supply high input voltage, two-switch Flyback converter was proposed to use high side and low side 800V Si MOSFETs as shown in Fig.1, but it has the additional isolation gate drive circuit which increases component counts and complicates the design. This application note proposes a single-end Flyback converter to replace complicated two-switch Flyback converter by using 1700V SiC MOSFET. An active start-up circuit is also introduced to achieve less start-up losses with faster start up time. The 60W experimental reference design demonstrates that the 1700V SiC MOSFET can reduce total cost and simplify the design of auxiliary power supply.

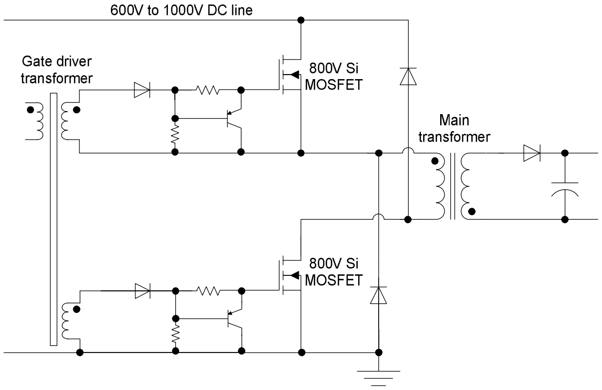

3. Cree 1700V SiC MOSFET

Today, SiC devices are characterized by a number of promising properties like high rating voltages, low switching losses, low on-state resistance, higher operating temperature, and high radiation hardness. A commercially available 1700V TO-247 packaged SiC MOSFET, C2M1000170D, from Cree Inc is used for a wide input auxiliary power supply application. The table compares the key parameters between SiC MOSFET and Si MOSFET with common TO-247 package. From this comparison, SiC MOSFET can support much higher blocking voltage to 1700V and avalanche voltage above 1800V, while Si MOSFET only has 1500V blocking voltage with lower avalanche voltage. For the on-state resistance and parasitic capacitance, the SiC MOSFET has lower value than Si MOSFET to have low conduction losses and low switching losses. This key difference will value 1700V SiC MOSFET to have high efficiency and high reliability replacing 1500V Si MOSFET.

Table 1: Parameter comparisons of 1700V SiC MOSFET and 1500V Si MOSFET

Parameters	**SiC MOSFET** **C2M1000170D**	**Si MOS** **STW4N150**	**Si MOS** **2SK2225DS**
V(BR)DSS	1700V	1500V	1500V
Avalanche	>1800V	N/A	N/A
Id @ Tc=25°C	5A	4A	2A
Rdson @150°C	2ohm	9ohm	20ohm
Coss	14pF	120pF	60pF
Tjmax	>150°C	150°C	150°C
Package	TO-247	TO-220, TO-247	TO-3PF

4. ACTIVE START-UP CIRCUIT

In this design, a non-dissipative, active start-up circuit has been implemented to optimize converter efficiency and fast start-up time. The alternative is to use a pure resistive start-up circuit which significantly affects converter efficiency and start up times at low input voltages in a negative way. Figure 2 shows the proposed active start-up circuit. When input voltage is increasing, Q6 is turned on by Vbase from path R31 to R36. The VCC voltage comes from path R22 to R25 when U1 (UCC28C44) is turning on. Once U1 starts operating, the VCC supply comes from the primary auxiliary winding. When VCC reaches the startup threshold of U1, the VREF (+5V) goes to high and Q7 is turned on. And then Q6 is turned off, which disconnects the start-up current path to VCC. The R31 to R36 resistors with large value are used as the voltage balancing for input capacitors C1 to C3. The startup resistors R22 to R25 feeds the PWM controller of U1 until the auxiliary supply voltage rises and is disconnected from VCC of U1 and then there are no more losses from start-up resistors. So the active start-up circuit can reduce the start up power dissipation, especially at high line input voltage and improve the efficiency. The additional power dissipation under such normal steady state conditions is due to the balance resistances, and they can be set at very high values (>6Mohm). More importantly, due to low resistance values for this active start-up circuit, the start-up time will be short and can be trimmed to meet targeting start-up time. If assuming minimum start-up time 1s, the VCC capacitance can be calculated as follows:

$$C_{start-up} > \frac{I_{UCC28C44start-up}T_{start-up}}{V_{UVLO\_on} - V_{UVLO\_off}} \qquad (1)$$

From datasheet of UCC28C44: $I_{UCC28C44start-up} < 0.1mA$; $V_{UVLO\_on} = 14.5V$; $V_{UVLO\_off} = 9.0V$. If $C_{Start-up} > 18\mu F$, it can select the VCC capacitance is 22uF. The total start-up current may then be calculated using the below equation:

$$I_{start-up} = \frac{C_{start-up} V_{UVLO\_on}}{T_{start-up}} = \frac{22\mu F \cdot 14.5V}{1S} = 0.319mA \qquad (2)$$

Hence, the total start-up resistors (R22 to R25) may be calculated as:

$$R_{start-up} = \frac{V_{DC\min} - V_{UVLO\_off}}{I_{start-up}} = \frac{200V - 9V}{0.319mA} = 600K\Omega \qquad (3)$$

Assuming worse darlington gain h_{FE} is 500, the total balance resistance (R31-R36) may be calculated as:

$$R_{Balance} = \frac{V_{DC\min} - V_{UVLO\_off}}{I_{start-up} / h_{FE}} = \frac{200V - 9V}{0.319mA} < 300M\Omega \qquad (4)$$

By using much higher balance resistance, total additional losses can be seen to have no negative impact on total losses.

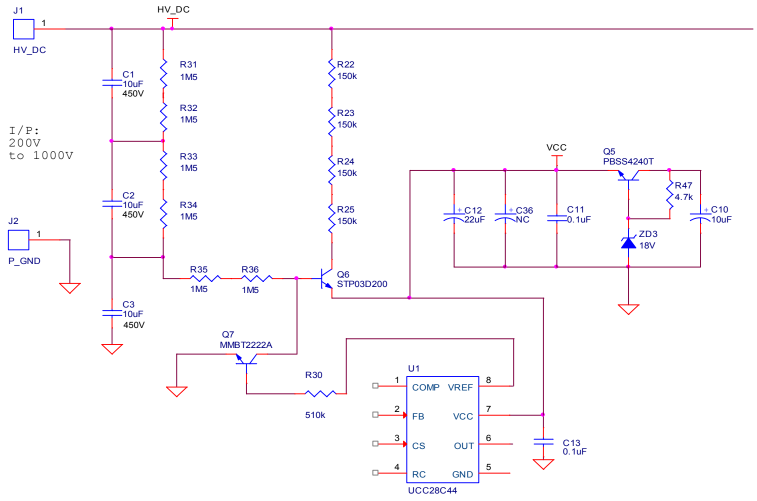

Figure 2: The proposed active start-up circuit

5. EXPERIMENTAL RESULTS

To demonstrate high performance of 1700V SiC MOSFET, a 60W single-end Flyback auxiliary power supply with proposed active start-up circuit is developed as shown in Figure 3.

Table 2: 60W auxiliary SMPS prototype design specification with 1700V SiC MOSFET

Input Voltage	200Vdc to 1000Vdc		
Output Voltage	+12Vdc	+5Vdc	-12Vdc
Output Current	4.5A	0.5A	0.25A
Frequency	75KHz		
Efficiency	>83%		

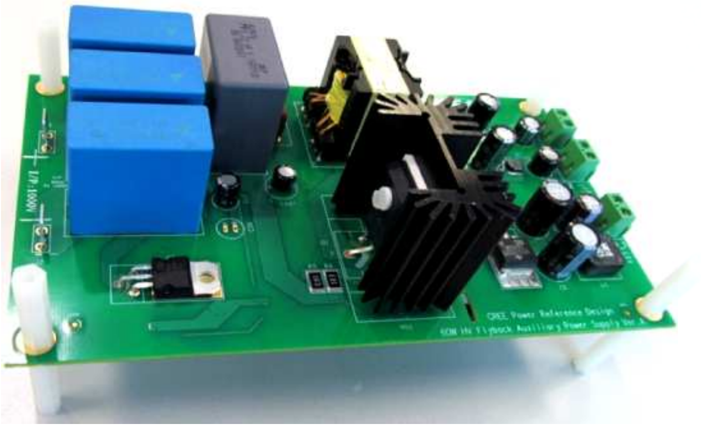

Figure 3: Photo of 60W auxiliary SMPS with 1700V SiC MOSFET

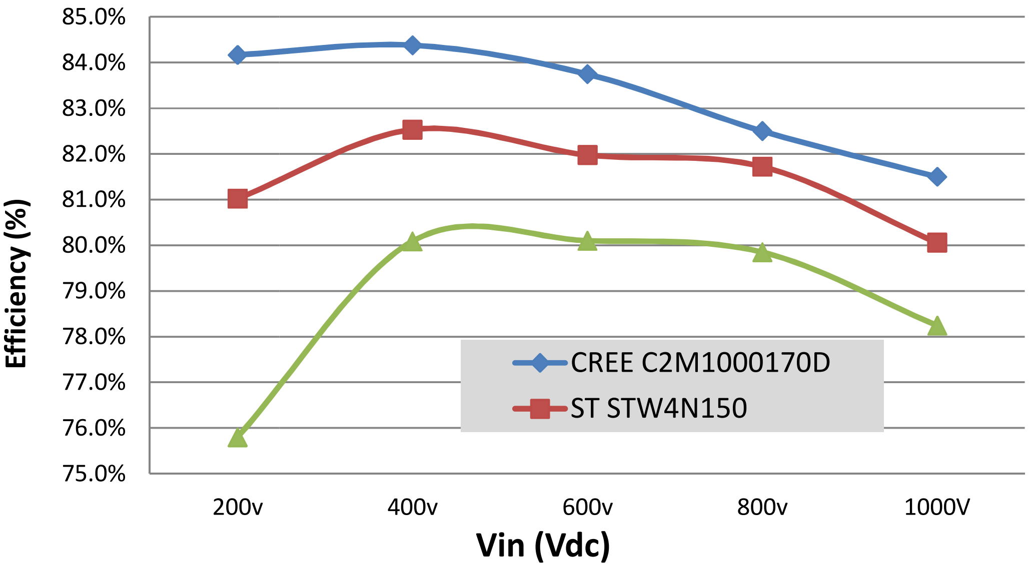

Figure 4: 60W auxiliary SMPS efficiency with 1700V SiC MOSFET

Figure 4 compares measured efficiency at full load with input voltage varying from 200V to 1000V using different Si and SiC devices. Due to lower on-state resistance and parasitic capacitance, the 1700V SiC MOSFET can achieve a higher efficiency when compared to other 1500V Si MOSFET competitors. Thermal comparison at full load with the same heat sink is shown in Fig.5, SiC MOSFET clearly shows a lower operating temperature at 45.9°C when compared to Si 1500V MOS at 60°C and 99.9°C. It shows that 1700V SiC MOSFET can achieve higher reliability. Use of the 1700V SiC MOSFET also allows us to use a small low cost heat sink due to the fact that a smaller amount of heat needs to be dissipated as shown in Figure 6. This can save the auxiliary power board size and improve power density.

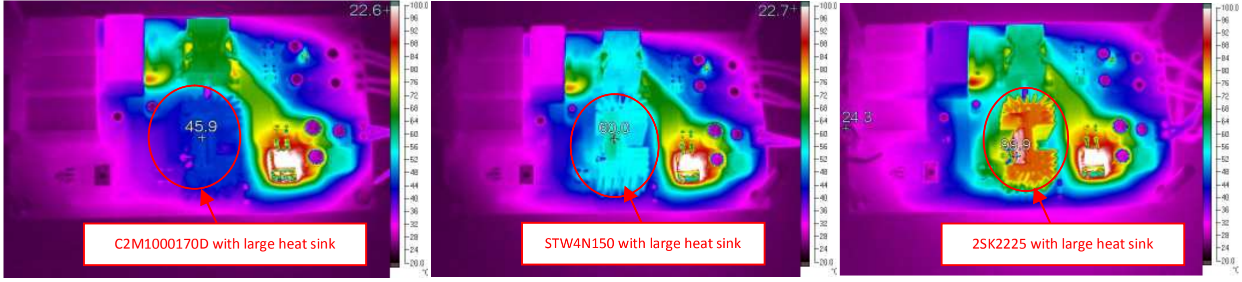

(a) SiC MOS C2M1000170D (b) Si MOS STW4N150 (c) Si MOS 2SK2225

Figure 5: Thermal comparison with same large heat sink and input voltage is 1000Vdc

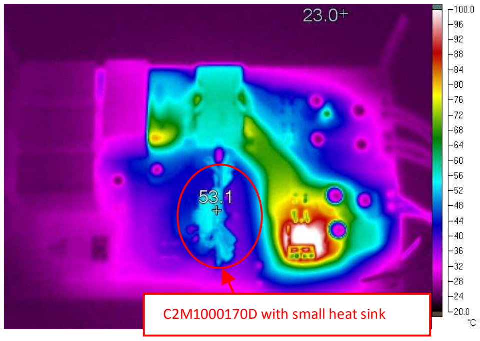

Figure 6: SiC MOSFET Thermal with small low cost heatsink and input voltage is 1000Vdc

Figure 7 shows the start up waveform with the proposed active start-up circuit. At 1000Vdc input, start up time is less 100ms and at 200Vdc input, start up time is less than 1s. Meanwhile, by trimming the start-up resistor R22 to R25, it can achieve faster start up time smoothly without sacrificing efficiency.

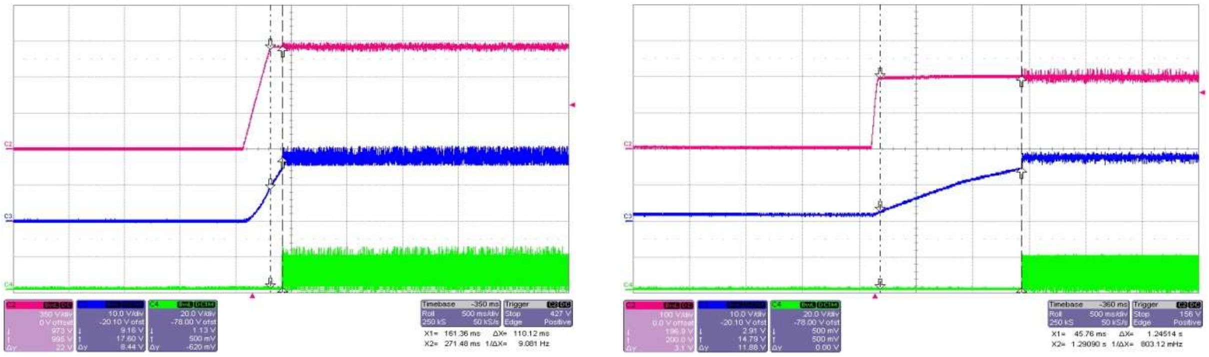

(a) 1000V input full load (b) 200V input full load

Figure 7: Start-up sequence waveforms

C2 (pink): Vin, 350V/Div; C3 (blue): Vcc, 10V/Div; C4 (green):Vgs, 20V/Div

Figure 8 shows the Vgs and Vds waveforms at difference input voltage and output loading (full load and light load). It shows that 1700V SiC MOSFET Vgs and Vds waveforms are very clean with fast switching at 200Vdc and 1000Vdc inputs.

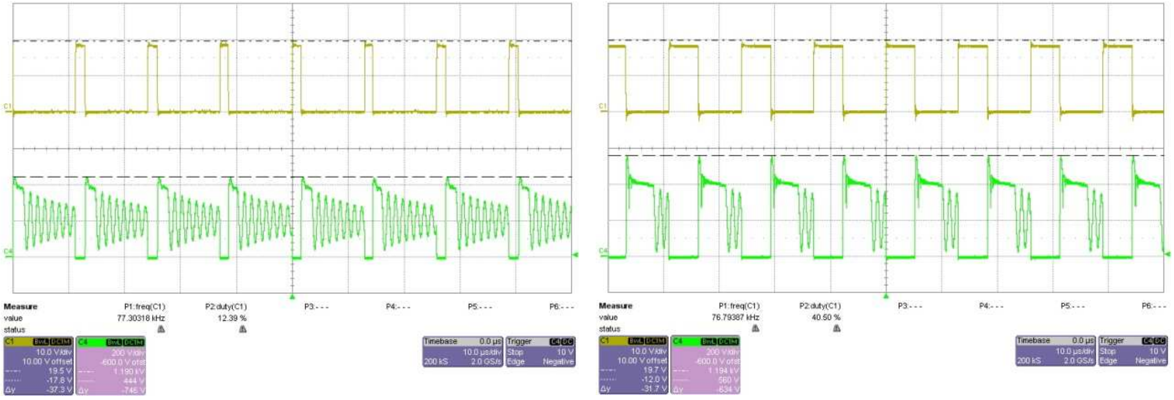

(a) Input: 200Vdc, Light load

(b) Input: 200Vdc, Full load

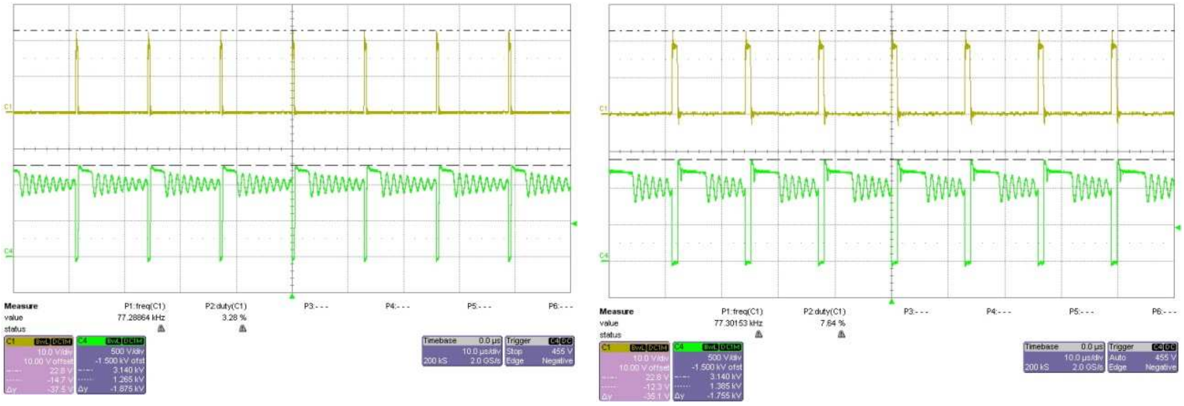

(c) Input: 1000Vdc, Light load

(d) Input: DC 1000V, Full load

Figure 8: Vgs and Vds waveforms of 1700V SiC MOSFET

C1(yellow): Vgs, 10V/div; C4 (green): Vds, 500V/div

REFERENCES

[1] C2M1000170D 1700V SiC MOSFET datasheet, *Cree InC.*
[2] JinBin Zhao, and FengZhi Dai, “Soft-switching two-switch flyback converter with wide range,” in *Industrial Electronics and Application, 2008. ICIEA 2008.*
[3] Robert W, Dragan M, Fundamentals of Power Electronics, *Boulder Colorado, 2002.*

Appendix A – Schematic

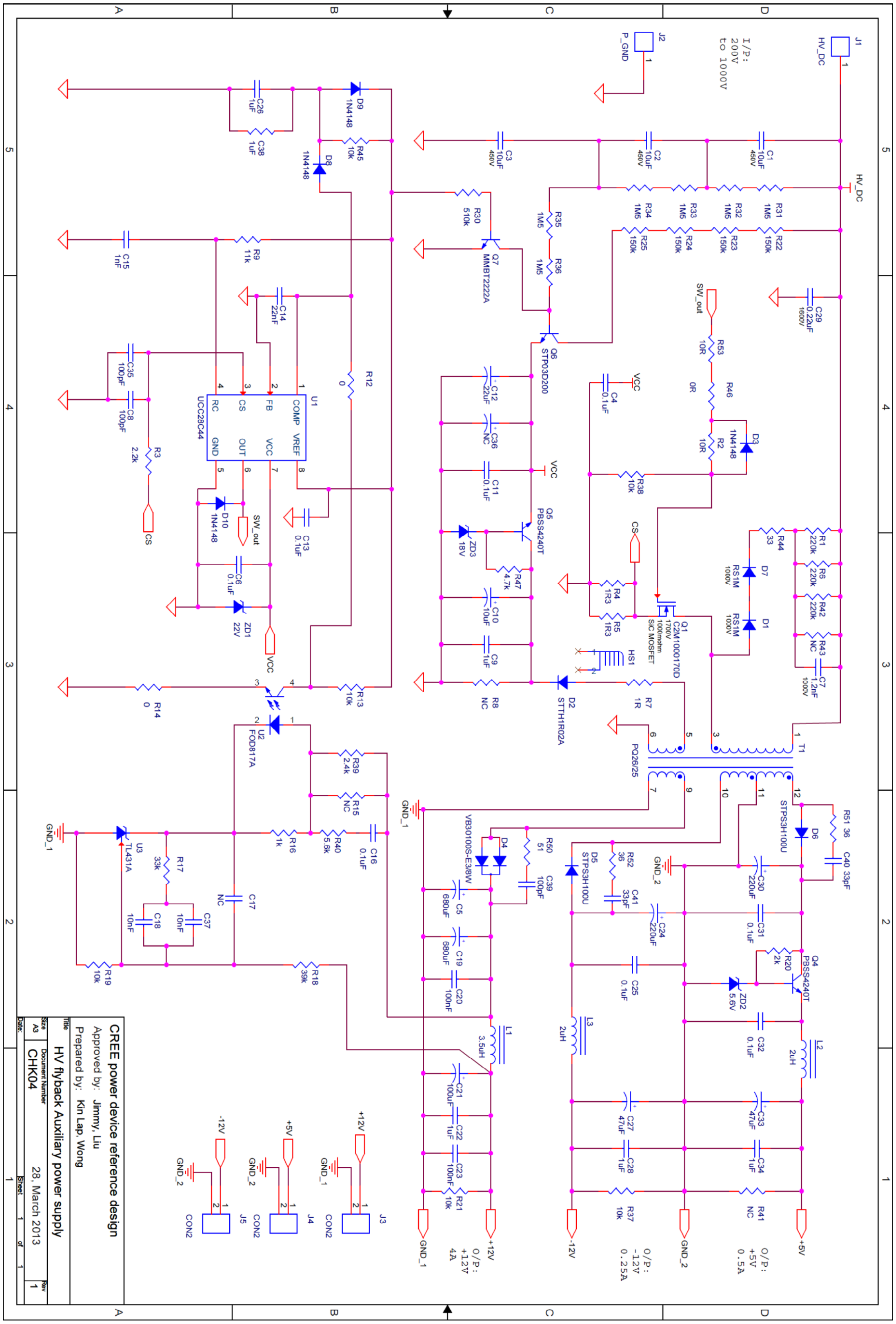

Appendix B - BOM

	Part no.	Value	Manufacturer Part no.	Manufacturer name	Description
1	C1	10uF	B32794D2106K	EPCOS	MKP, 5%
2	C2	10uF	B32794D2106K	EPCOS	MKP, 5%
3	C3	10uF	B32794D2106K	EPCOS	MKP, 5%
4	C4	0.1uF			CAP CER 100V 10% X7R 0603
5	C5	680uF	EEU-HD1V681	Panasonic	
6	C6	0.1uF			CAP CER 100V 10% X7R 0603
7	C7	1.2nF	ECW-H16122JV	Panasonic	
8	C8	100pF			CAP CER 100V 10% X7R 0603
9	C9	1uF			CAP CER 100V 10% X7R 1206
10	C10	10uF	ECEA1HKS100	Panasonic	
11	C11	0.1uF			CAP CER 100V 10% X7R 1206
12	C12	22uF	EEA-GA1V220	Panasonic	
13	C13	0.1uF			CAP CER 100V 10% X7R 0603
14	C14	22nF			CAP CER 100V 10% X7R 0603
15	C15	1nF			CAP CER 100V 10% C0G 0603
16	C16	0.1uF			CAP CER 100V 10% X7R 0603
17	C17	NC			
18	C18	10nF			CAP CER 100V 10% X7R 0603
19	C19	680uF	EEU-HD1V681	Panasonic	
20	C20	100nF			CAP CER 100V 10% X7R 0603
21	C21	100uF	UPB1V101MPD	Nichicon	
22	C22	1uF			CAP CER 50V 10% X7R 0603
23	C23	100nF			CAP CER 100V 10% X7R 0603
24	C24	220uF	EEU-EB1V221	Panasonic	
25	C25	0.1uF			CAP CER 100V 10% X7R 0603
26	C26	1uF			CAP CER 50V 10% X7R 0603
27	C27	47uF	EEA-GA1V470	Panasonic	
28	C28	1uF			CAP CER 50V 10% X7R 0603
29	C29	0.22uF	R76TR3220SE30K	Kamet	
30	C30	220uF	EEU-EB1V221	Panasonic	
31	C31	0.1uF			CAP CER 100V 10% X7R 0603
32	C32	0.1uF			CAP CER 100V 10% X7R 0603
33	C33	47uF	EEA-GA1V470	Panasonic	
34	C34	1uF			CAP CER 50V 10% X7R 0603
35	C35	100pF			CAP CER 100V 10% X7R 0603
36	C36	NC			
37	C37	10nF			CAP CER 100V 10% X7R 0603
38	C38	1uF			CAP CER 50V 10% X7R 0603
39	C39	100pF			CAP CER 100V 10% C0G 1206
40	C40	33pF			CAP CER 100V 10% C0G 1206
41	C41	33pF			CAP CER 100V 10% C0G 1206
42	D1		RS1M-13-F	Diodes	
43	D2		STTH1R02A	ST	
44	D3		1N4148		
45	D4		VB30100S-E3/8W	Vishay	
46	D5		STPS3H100U	ST	
47	D6		STPS3H100U	ST	
48	D7		RS1M-13-F	Diodes	
49	D8		1N4148		
50	D9		1N4148		
51	D10		1N4148		
52	J1	HV_DC	2 pin, P:5.08mm		HV tips terminal
53	J2	P_GND	2 pin, P:5.08mm		HV tips terminal
54	J3	CON2	282837-2	TE	Horizontal, P:5.08mm
55	J4	CON2	282837-2	TE	Horizontal, P:5.08mm
56	J5	CON2	282837-2	TE	Horizontal, P:5.08mm
57	L1	3.5uH	744771003	Wurth	
58	L2	2.7uH	SWPA5020S2R7NT	Sunlord	
59	L3	2.7uH	SWPA5020S2R2NT	Sunlord	
60	Q1	**1000mohm, 1700V**	**C2M1000170D**	**CREE**	**1700V, 1000mohm, SiC MOSFET**
61	Q4		PBSS4240T	NXP	

62	Q5		PBSS4240T	NXP	
63	Q6		STP03D200	ST	
64	Q7		MMBT2222A		
65	R1	220K			1W, 1%
66	R2	10R			RES, 0.25W, 1%, 1206
67	R3	2k2			RES, 0.25W, 1%, 1206
68	R4	1R3	CRCW25121R30FP	Vishay	1W, 1%
69	R5	1R3	CRCW25121R30FP	Vishay	1W, 1%
70	R6	220K			1W, 1%
71	R7	1R			RES, 0.25W, 1%, 1206
72	R8	NC			
73	R9	11k			RES, 0.1W, 1%, 0603
74	R12	0			RES, 0.1W, 1%, 0603
75	R13	10k			RES, 0.1W, 1%, 0603
76	R14	0			RES, 0.1W, 1%, 0603
77	R15	NC			
78	R16	1k			RES, 0.1W, 1%, 0603
79	R17	33k			RES, 0.1W, 1%, 0603
80	R18	39k			RES, 0.1W, 1%, 0603
81	R19	10k			RES, 0.1W, 1%, 0603
82	R20	2K			RES, 0.1W, 1%, 0603
83	R21	10k			RES, 0.25W, 1%, 1206
84	R22	150k			RES, 0.5W, 200V, 1%
85	R23	150k			RES, 0.5W, 200V, 1%
86	R24	150k			RES, 0.5W, 200V, 1%
87	R25	150k			RES, 0.5W, 200V, 1%
88	R26	0R			RES, 0.5W, 200V, 1%
89	R27	0R			RES, 0.5W, 200V, 1%
90	R28	0R			RES, 0.5W, 200V, 1%
91	R29	0R			RES, 0.5W, 200V, 1%
92	R30	510K			RES, 0.25W, 1%, 1206
93	R31	1M5			RES, 0.5W, 200V, 1%
94	R32	1M5			RES, 0.5W, 200V, 1%
95	R33	1M5			RES, 0.5W, 200V, 1%
96	R34	1M5			RES, 0.5W, 200V, 1%
97	R35	1M5			RES, 0.5W, 200V, 1%
98	R36	1M5			RES, 0.5W, 200V, 1%
99	R37	10k			RES, 0.25W, 1%, 1206
100	R38	10k			RES, 0.25W, 1%, 1206
101	R39	2.4k			RES, 0.1W, 1%, 0603
102	R40	5.6k			RES, 0.1W, 1%, 0603
103	R41	NC			
104	R42	220K			1W, 1%
105	R43	220K			1W, 1%
106	R44	33			RES, 0.5W, 200V, 1%
107	R45	10k			RES, 0.1W, 1%, 0603
108	R46	0			RES, 0.5W, 100V, 1%
109	R47	4.7k			RES, 0.1W, 1%, 0603
110	R50	51R			RES, 0.25W, 1%, 1206
111	R51	36R			RES, 0.25W, 1%, 1206
112	R52	36R			RES, 0.25W, 1%, 1206
113	R53	10R			RES, 0.25W, 1%, 1206
114	T1	PQ26/25	750341672	Würth-midcom	PQ2625 transformer
115	U1	UCC28C44	UCC28C44D	TI	
116	U2	FOD817A	FOD817ASD	Fairchild	
117	U3	TL431A	TL431AIDBZ	TI	
118	ZD1	22V	MMSZ5251	Vishay	0.5W
119	ZD2	5.6V	MMSZ5232	Vishay	0.5W
120	ZD3	18V	MMSZ5248	Vishay	0.5W
121	HS1		RA-T2X-38E	Ohmite	Heatsink

Appendix C – PCB layout

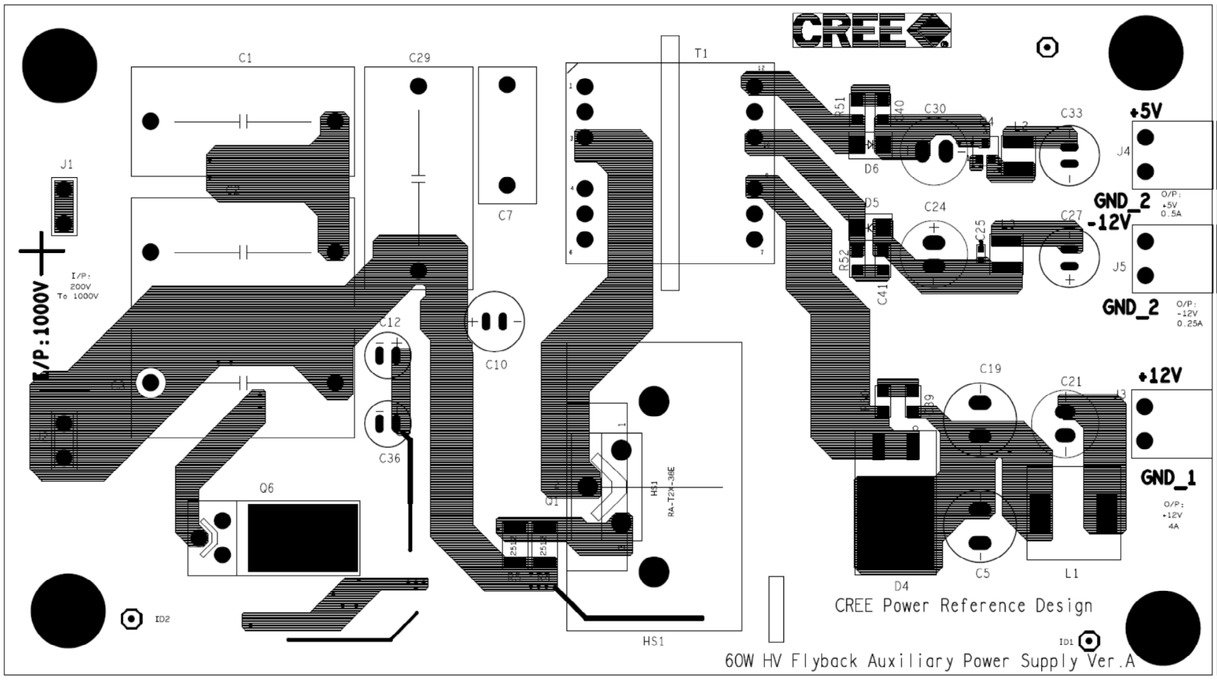

Top side PCB layout

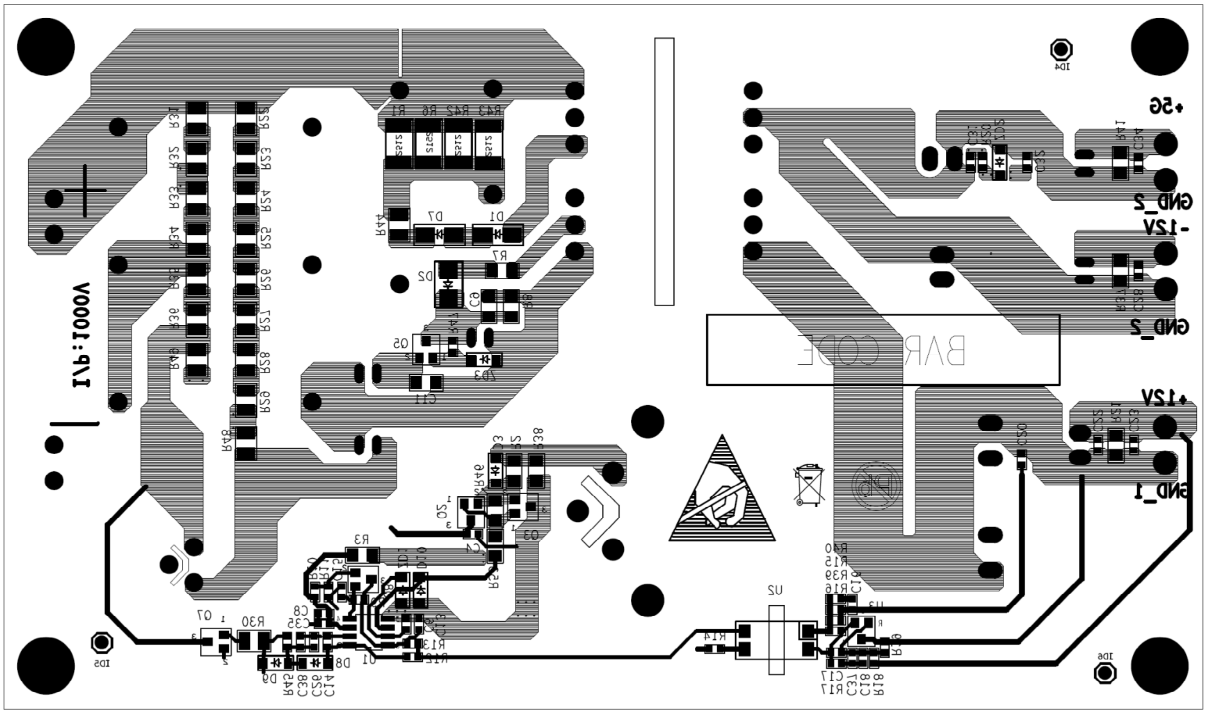

Bottom side PCB layout